Vol 14 No 7, July 2005
1009-1963/2005/14(07)/1277-05

Chinese Physics

© 2005 Chin. Phys. Soc.
and IOP Publishing Ltd

Studies of the beam finding and targeting accuracy of the CAS–LIBB single-particle microbeam*

Wang Xiao-Hua(王晓华), Wang Xu-Fei(王旭飞), Hu Zhi-Wen(胡智文),
Cheng Lian-Yun(陈连运), Zhang Jun(张 俊), Zhan Fu-Ru(詹福如),
Li Jun(李 军), Chen Bin(陈 斌), Xu Ming-Liang(许明亮),
Wu Li-Jun(吴李君), Wang Shao-Hu(王绍虎), and Yu Zeng-Liang(余增亮)†

Key Laboratory of Ion Beam Bioengineering, Institute of Plasma Physics, Chinese Academy of Sciences, and the Key Laboratory of Ion Beam Bioengineering in Anhui Province, Hefei 230031, China

(Received 29 October 2004; revised manuscript received 12 January 2005)

A single-particle microbeam facility has been constructed at the Key Laboratory of Ion Beam Bioengineering (LIBB), Chinese Academy of Sciences (CAS). The system was designed to deliver a defined number of hydrogen ions produced by a Van de Graaff accelerator, in an energy range of 2.0–3.0MeV, into an area smaller than the nuclei of individual living cells grown on thin plastic films. The beam is collimated by a borosilicate glass capillary that forms the beam-line exit. An computer integrated control program is developed to recognize the cells and to target them one by one for irradiation.

Experiments for finding (capturing and recognizing) the microbeam position in the microscope imaging system and measuring the overall targeting accuracy of the facility are presented in this article. When a borosilicate glass capillary with 5μm inner diameter and 980μm length is used as the microbeam collimator, the overall targeting accuracy is that 91% aimed pit clusters are located within 2.4 μm radius, and 98% are within 3.6 μm radius.

Keywords: single-particle microbeam, borosilicate glass capillary, CR-39, targeting accuracy
PACC: 0150P, 2921, 0777, 8780

1. Introduction

Microprobes for the study of radiation damage to biological systems have been known since the 1950s.[1] However, they were not used extensively until a recent resurgence of interest[2−4] due in part to recent developments in computer-based microscopy systems that allow rapid location and accurate positioning of target cells.[5−8]

Microbeam offers a unique method for selecting and irradiating individual cells with a defined number of charged particle.[9−13] That makes the microbeam an exquisite tool for radiobiological researches to simulate low dose environmental irradiation. For a microbeam to truly fulfil its role in modern radiobiology, it must excel in two key technical parameters: the single particle detecting efficiency and the microbeam targeting accuracy. The particle detecting efficiency has been reported in Refs.[14,15]. This paper mainly focuses on the studies of the beam finding and the targeting accuracy of the CAS-LIBB (Key Laboratory of Ion Beam Bioengineering, Chinese Academy of Sciences) single-particle microbeam.

2. Beam finding

Collimated protons accelerated by a 5.5MeV Van de Graaff accelerator[7,16] are used to irradiate individual living cells. For irradiation, cells are grown on a specially designed dish consisting of a 3.5μm thick Mylar film. The cell dish is mounted on a sample stage (Märzhäuser, Wetzlar GmbH, Germany) driven by stepping motors. A computer-controlled charge-coupled device (CCD) camera (CCD-72E, Dage-MTI, Michigan City, USA), a variable-gain image intensifier

*Project supported by the National Major Technologies R&D Program of China during the 10th Five-Year Plan Period (Grant No 2001BA302B-01), the magnitude instrument developing project of Chinese Academy of Sciences, Ministry of Agriculture "948" Project, the National Science Foundation of China (Grant No 19875054), and the National Science Fund for Distinguished Young Scholars, China (Grant No 10225526).

†Corresponding author. E-mail: zlyu@ipp.ac.cn

(GenIISys, Dage-MTI, Michigan City, USA), and a fluorescent microscope (Olympus BX2, Japan) jointly perform to scan the cells in the dish. Then an image analysis program automatically finds and records the position of each stained cell. These components compose the image analysis system of the microbeam facility (as shown at the top of Fig.1). To irradiate cells, the microscope objective is replaced with a photomultiplier tube that detects[17] photon pulses produced when a particle traverses a thin scintillator (BC400) situated between the collimator and the cell dish. Thereafter, every cell is precisely positioned over the beam exit and exposed to a chosen number of protons automatically. The schematic diagram of the microbeam facility and the integrated control system is shown in Fig.1.

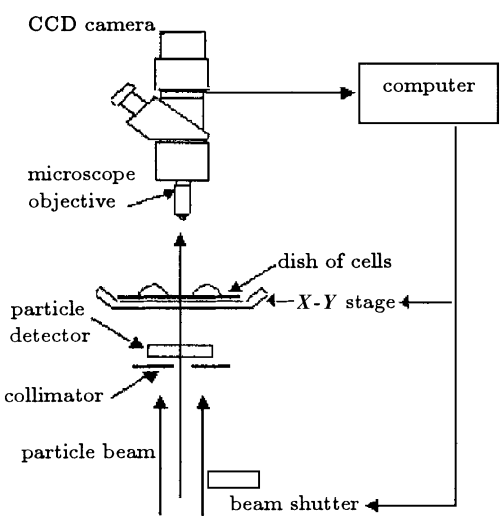


Fig.1. Schematic drawing of the microbeam facility and the integrated control system.

The overall targeting accuracy of a microbeam system is limited not only by the properties of the collimator, but also by the accuracy with which the cells can be aligned relative to the microbeam. A 980μm-long borosilicate glass capillary with a 5μm bore is mounted at the end of the beam line as the microbeam exit. To align cells relative to the beam accurately, it is required that the beam position should firstly be found and determined as the origin of coordinates in the image analysis system (i.e., the so-called beam finding step). Basing on this origin, every cell can then be moved one by one to the beam position by the motorized stage.

The borosilicate glass capillary collimator with 5μm bore is mounted at the beam line exit and capped with a 3.5μm Mylar vacuum film. After the Mylar is a 7μm aluminium foil as photon reflector (for shielding the spurious photons from underside entering the photomultiplier window), and an 18μm thick scintillator (Bicron BC400). At the end they are all packed with another 3.5μm Mylar (the details are shown in Fig.2). The beam position is identified by visualizing the light spot produced when particles hit the scintillation foil. Using the Matrox Imaging Library package (Matrox Electronic Systems, Dorval, Canada), a dedicated image analysis program has been developed to acquire the CCD pixel signals of the fluorescent spot and to analyze the spatial distribution of the particles, thus to determine the exact microbeam position in the image analysis system.

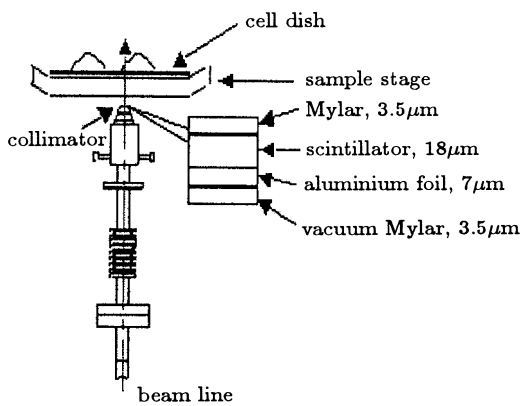


Fig.2. The layout of the substances that particles pass prior to the beam exit.

Figure 3 is a typical image of the fluorescent spot produced in the scintillator (BC400) by the particle beam (3.0MeV protons beam with 500 particles per second, 5μm collimator, 18μm BC400, and 1 second integration). Generally, 10–20 frames of the fluorescent spot images are picked up by the image analysis system, and the gray value of each pixel in every image is calculated. Then the brightest pixels in the fluorescent spot of each image are selected. Their corresponding coordinates (relative to the top-left corner, that is, the origin of coordinates is at the top-left corner) are used to determine the microbeam position by the appearance probabilities of these coordinates. An analysis result of 10 frames of spot images in Fig.4 showing that 4 results are coordinates (418,344), and 3 of them (419,344). That is, the probability of the coordinates (418,344) is 40%, and the probability of the coordinates (419,344) is 30%. Based on the probabilities and the average of these coordinates in Fig.4, the beam position coordinates are calculated to be (418,344). Using the calculated beam position, coordinates of cells are transferred relative to the beam point (regarded as origin of coordinates) and each cell

is moved to the microbeam exit for irradiation. As an important factor for the targeting accuracy in the microbeam system, the beam finding ability will be evaluated in the following tests of the overall targeting accuracy.

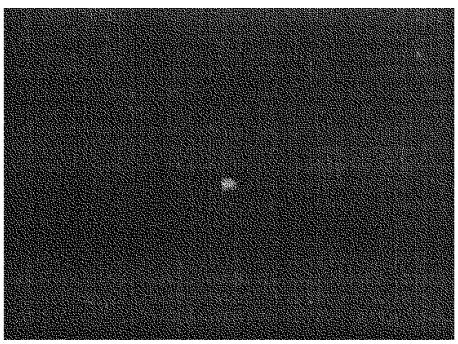


Fig.3. An image of the spot of light produced within the scintillation foil by the particle beam.

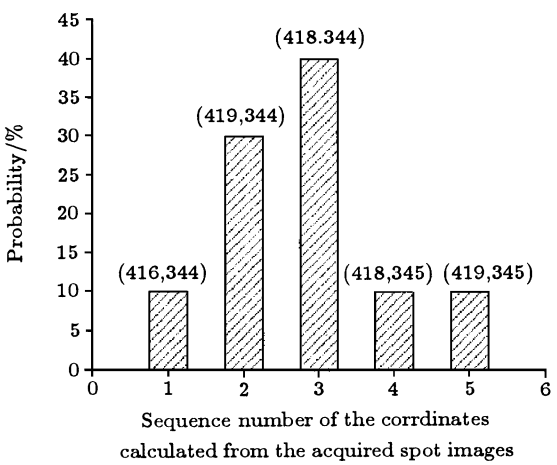


Fig.4. Probabilities of the beam position coordinates calculated from the acquired spot images.

3. Overall targeting accuracy of the microbeam

Generally, there are two key parameters contributing to the overall targeting accuracy of the microbeam: (1) spatial distribution of the collimated particles at the beam exit, and (2) the abilities of the integrated control system to recognize the targets, to record their positions and to move each target to the microbeam exit precisely.

3.1. Beam collimation

Nuclear track-etch detectors are extensively used to assess the performance of microbeam facilities. CR-39 plastic detector (flake shape, 10mm×10mm×1mm) has been employed to log every particle impact point and quantify the extent to which particles are scattered off-axis at the sample position for certain collimator assemblies. The targeting accuracy of the collimator is evaluated by exposing a CR-39 detector (attached on the cell dish) to the beams at the sample position. After irradiation, CR-39 detector is etched in 6×10^3mol/m^3 NaOH at 70°C for about 2 to 2.5h, depending on the linear energy transfer of the ions. The tracks of the ions are visualized as micrometer-size pit clusters on the surface of the CR-39 detector, and the spatial distribution of etched ion tracks is observed by the image analysis system. Using 2.0–3.0MeV proton ions and a 5μm diameter by 980μm long borosilicate glass capillary collimator, the testing results show that more than 91% of the pit clusters (100 protons in each pit cluster, totally 500 pit clusters have been analyzed) are smaller than 6.8μm in diameter, and 95% of the particles are within 3μm of the mean hitting position. Figure 5 shows a 10×10 grid etched by the CAS–LIBB microbeam, with 100 particles at each grid point.

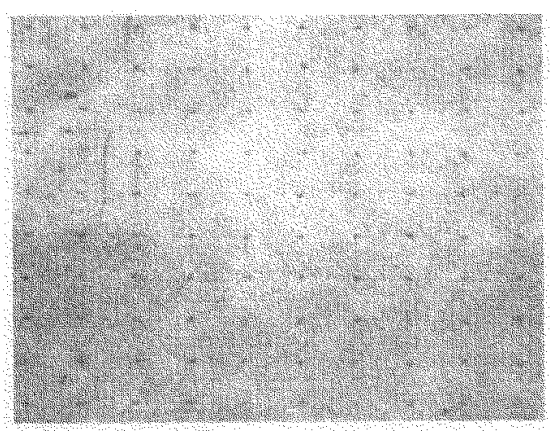


Fig.5. A 10×10 grid etched on CR-39 by the CAS–LIBB microbeam with 100 particles at each grid point.

3.2. Overall targeting accuracy measurement

Besides the beam collimation, a complete evaluation of the overall targeting accuracy requires other relevant aspects as well, such as the beam finding accuracy, the automated cell-finding and positioning accuracy of the image analysis system, and the target-locating accuracy of the motorized sample stage. In our facility, we adopt a method developed by the Gray Laboratory group and published in Ref.[18].

Firstly, a data file of coordinates, generally a 10×10 grid with 100μm spacing between neighbours is generated. Then the data is used to move the motorized stage automatically, and a pre-defined num-

ber (50 or 100) of particles are delivered to each grid point. After etching in NaOH, a microarray of pit clusters produced by the particles from the microbeam is formed on the CR-39 track detector film. When each grid point is irradiated by 100 proton ions, each pit cluster at these grid points appears as a single pit cluster about 6μm in diameter. Here, these irradiated pit clusters can be made to simulate the cells during a second exposure of the detector, such that the video signal is captured by a Matrox Genesis image processing board using the Matrox Imaging Library. A program written in Visual Basic under the Windows NT operating system controls the motorized stage motion and the image analysis system.[19,20] After the image of the pit clusters is captured, a threshold in intensity is set to separate the etched clusters from the background and the central coordinates of each pit cluster are calculated using the control program.

The second exposure of the CR-39 detector is a "cluster-inserting" test by inserting new pit clusters into the mid-point between the adjacent pre-etched clusters. The overall targeting accuracy, which reflects the capability of the system to align the target and the beam properly, is evaluated by measuring the discrepancy between the actual irradiation pit cluster and the expected position. Note that it is actually the midpoint between adjacent pit clusters that is targeted; otherwise, a "direct hit" over the pre-etched clusters would not be apparent when the detector is etched for the second time. To obtain the data file of the mid-point coordinates for driving the motorized stage motion in the new "inserting irradiation", coordinates of the mid-points of either two or four adjacent pit clusters are calculated based on the recorded coordinates of the irradiated pit clusters in the first exposure. But before the motorized stage is moved to the beam exit automatically, the coordinates of the midpoints need to be transferred relative to the beam exit point (which has been recorded in the beam finding step). Each mid-point is then positioned over the beam exit by the motorized sample stage automatically to be irradiated.

Figure 6 is an example of the CR-39 image after two irradiations. 100 protons were delivered to each mid-point (between adjacent pit clusters formed in the first irradiation). The smaller pit clusters are the "inserted" clusters, while the larger ones are the pre-etched clusters (they are larger than the inserted clusters because they were etched twice in NaOH). By analyzing the pit clusters in Fig.6, the results (in Fig.7) show that 98% of the inserted pit clusters are located within the discrepancy of 3.6μm from the desired mid-point position, and 91% of the inserted clusters are located within the discrepancy of 2.4μm. The performance could be further improved by reducing the air gap between the beam exit and the target position. The air gap reducing could be realized using a recently improved automatic sample stage with the ability of precise Z-axis motion (in addition to the X-axis motion and Y-axis motion), which can move the culture dish to an irradiation position as close as possible to the beam exit and move it slightly away during the drive movement.

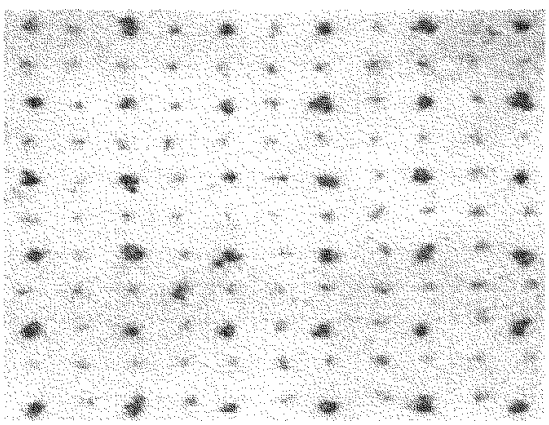


Fig.6. A typical CR39 image after two etches used to assess the overall targeting accuracy.

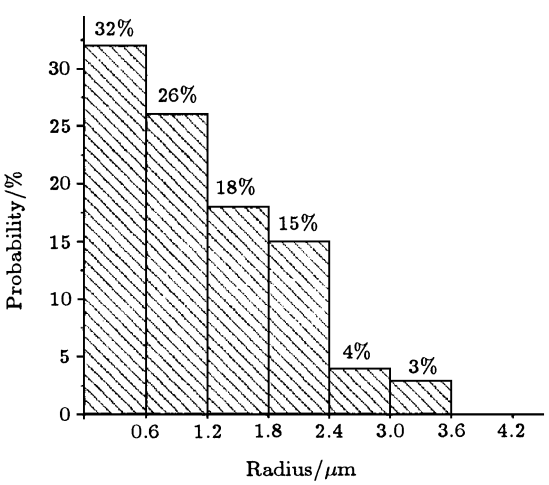


Fig.7. Overall targeting accuracy of the microbeam system. The performance of beam finding, video identification, and sample stage motion are included.

4. Results and discussion

From the experimental researches discussed above, when the borosilicate glass capillary of 5μm inner diameter is employed as microbeam collimator, the

measurement results show that 95% of the delivered particles are located within 3μm radius area. With the performance of beam finding, video identification, and sample stage motion, an overall targeting accuracy has been achieved that 98% inserted pit clusters are located within 3.6μm of the desired position, and 91% are within 2.4μm of the desired position. Considering the common size for mammalian cells (about 10–50μm) used for radiobiological researches in the laboratory, the microbeam targeting accuracy is sufficient for irradiation of individual cells.

From the outset, the CAS–LIBB microbeam has been in a constant state of evolution. A number of aspects including increasing the cell throughput, the targeting accuracy, the penetration of the radiation, and the implementation of non-UV-radiation methods for target visualization are scheduled to be improved in the near future.

References

[1] Zirkle R and Bloom W 1953 *Science* **117** 487

[2] Geard C R, Brenner D J, Randers-Pehrson G and Marino S A 1991 *Nucl. Instrum. Meth.* B **54** 411

[3] Nelson J M, Brooks A L, Metting N F, Khan M A, Buschbom R L, Duncan A, Miick R and Braby L A 1996 *Radiat. Res.* **145** 568

[4] Folkard M, Vojnovic B, Prise K M, Bowey A G, Locke R J, Schettino G and Michael B D 1997 *Int. J. Radiat. Biol.* **72** 375

[5] Folkard M, Vojnovic B, Hollis K J *et al* 1997 *Int. J. Radiat. Biol.* **72** 387

[6] Folkard M, Vojnovic B, Gilchrist S *et al* 2003 *Nucl. Instrum. Methods* B **210** 302

[7] Randers-Pehrson G, Geard C R, Johnson G *et al* 2001 *Radiat. Res.* **156** 210

[8] Wu L J, Hei T K, Randers-Pehrson G *et al* 1999 *Nucl. Sci. & Tech.* **10** 143

[9] Hei T K, Wu L J, Liu S X *et al* 1997 *Proc. Natl. Acad. Sci.* USA **94** 3765

[10] Wu L J, Randers-Pehrson G, Xu A *et al* 1999 *Proc. Natl. Acad. Sci.* USA **96** 4959

[11] Geard C R, Randers-Pehrson G, Marino S A *et al* 2000 *Radiat. Res.* **153** 233

[12] Prise K M, Belyakov O V, Folkard M and Michael B D 1998 *Int. J. Radiat. Biol.* **74** 793

[13] Yu Z L 1997 *Physics* **26** 333

[14] Wang X F, Chen L Y, Yu Z L *et al* 2004 *Chin. Phys. Lett.* **21** 821

[15] Wang X F, Wang X H, Chen L Y, Hu Z W, Li J, Wu Y *et al* 2004 *Chin. Sci. Bull.* **49** 1806

[16] Yang H L *et al* 2004 *Acta Phys. Sin.* **53** 406 (in Chinese)

[17] Ouyang X P *et al* 2002 *Acta Phys. Sin.* **51** 1502 (in Chinese)

[18] Peng S, Folkard M, Gilchrist S, Locke R J, Yu Z and Michael B D 2001 *Nucl. Instrum. Methods* B **179** 145

[19] Wang X H, Wang S H and Yu Z L 2003 *Comput. Engin.* **29** 9 (in Chinese)

[20] Wang X H, Wang S H and Yu Z L 2003 *Comput. Engin.* **29** 35 (in Chinese)